# Electronic and crystal-field effects in the fine structure of electron energy-loss spectra of manganites

Weidong Luo,[1,2] Maria Varela,[2] Jing Tao,[3] Stephen J. Pennycook,[2] and Sokrates T. Pantelides[1,2]
[1]*Department of Physics and Astronomy, Vanderbilt University, Nashville, Tennessee 37235, USA*
[2]*Materials Science and Technology Division, Oak Ridge National Laboratory, Oak Ridge, Tennessee 37831, USA*
[3]*Department of Condensed Matter Physics and Materials Science, Brookhaven National Laboratory, Upton, New York 11973, USA*
(Received 10 November 2008; revised manuscript received 21 January 2009; published 23 February 2009)

The fine structure of oxygen-K electron energy-loss spectra (EELS) of transition-metal oxides is known to correlate with nominal oxidation states (NOSs) that are often interpreted as charge states. Here we report calculations of O-K EELS in $La_xCa_{1-x}MnO_3$ that agree with measured spectra and show that the variation in the prepeak's intensity with doping is controlled by the orbital occupancy of the majority-spin Mn 3*d* states, while its width is controlled by crystal-field splitting. The results confirm an earlier conclusion that the NOS extracted from EELS corresponds only to orbital occupancies, while the physical charge renders all atoms electrically neutral, even in so-called ionic crystals.

DOI: 10.1103/PhysRevB.79.052405 PACS number(s): 75.47.Lx, 71.20.Ps, 79.20.Uv

Transition-metal oxides (TMOs) have a wide range of structural, electronic, and magnetic properties and have attracted considerable interest.[1–5] The diverse properties arise largely because *d* shells of electrons offer greater flexibility than *p* shells in accommodating different oxidation states. Core-excitation spectra are widely used to probe the properties of TMOs, such as their chemical composition, electronic, and magnetic properties. More specifically, x-ray absorption and electron energy-loss spectroscopy (EELS) probe the unoccupied electronic states above the Fermi energy.[6–8] Thus, the trends in spectra have been used to extract oxidation states, the nature of charge ordering, and the magnetic moments.[9–15]

The oxygen-K EELS fine structure has provided especially fertile ground in such studies.[15–20] It has been found that the intensity of the first peak at threshold, universally called the "prepeak," correlates in a linear fashion with the Mn nominal oxidation state (NOS).[12–14] In a similar fashion, the energy separation between the first two peaks also correlates linearly with the Mn NOS.[14] The different NOS is usually viewed as transfer of actual physical charge from Mn to oxygen sites. For example, for a NOS of +4, usually denoted by $Mn^{4+}$, the usual interpretation is that there is a transfer of four physical charges from every Mn atom to the oxygen sublattice.

In a recent paper, however, we demonstrated that transition-metal (TM) atoms and O atoms in TMOs are in fact neutral.[21] The electron density around Mn atoms in various Mn oxides with different NOS is essentially the same and also the same as in Mn metal, where the NOS is zero. More specifically, a plot of the integrated electron density within a volume of radius *R* about any Mn atoms as a function of *R* is essentially indistinguishable in all cases. It is important to note that in the various environments, one has very different orbital occupancies; e.g., in Mn metal one has $3d^5$ occupancy whereas in the oxides the *d*-state occupancy is generally reduced. However, the "missing" charge is recovered from the oxygen occupancies because the oxygen orbitals overlap with the Mn sites significantly.

The net result is that the occupancies of individual orbitals do not translate into the actual physical charge associated with a given atom. The observed EELS trend has nothing to do with charge transfer or ionization of the TM atoms. It is intriguing that the orbital occupancies, as obtained from total-energy minimization in the actual calculations, always yield effectively neutral atoms. We can conclude that any departure from charge neutrality is energetically costly. Another recent study on TM atoms embedded in ionic and covalent host materials also concludes that the total charge around the TM atom remains almost unchanged when its oxidation state is altered.[22] The precise relationship among the O-K prepeak variations, orbital occupancies, and physical charge in manganites remains an open issue.

In this Brief Report, we report the results of a systematic study of O-K-edge EELS fine structures in $La_xCa_{1-x}MnO_3$ (LCMO) and their evolution as a function of doping *x*. The effects of both the solid state environment and the electron-hole interactions are included. The effect of the electron-hole interaction is small, whereby the O-K spectra truly probe the unoccupied Bloch states in the perfect crystal. The calculated spectra, specifically the prepeak intensities and peak separations, as functions of *x* are in excellent agreement with experimental data.[14] Detailed analysis of calculated spectra provides a comprehensive understanding of the fundamental origins of the observed trends. In particular, as previously noted,[6,11] the main peak in the spectra originates from a combination of the empty Ca 3*d* and La 5*d* states. More importantly, the evolution of the spectra as a function of doping is determined by two mechanisms: (a) the prepeak intensity is controlled virtually exclusively by variations of orbital occupancy in the Mn 3*d* $e_g$ majority-spin states; (b) the width of the prepeak is determined by the decreasing crystal-field splitting with increasing electron doping. The results clarify the nature of the measured O-K spectra in doped manganites, and features of the prepeak are traced back to electronic occupancy and crystal-field effects of the materials. The current work reconfirms that EELS probes the orbital occupancies, not the physical charge of the TM ions.[21] Finally, we show that the energy separation between the prepeak and the main peak has a true correlation with the doping parameter *x*,

 

which then relates to the nominal oxidation state $n$ because $n$ is defined by $n=4-x$.

Density-functional theory (DFT) (Refs. 23 and 24) with spin-polarized generalized-gradient approximation (GGA) (Ref. 25) as implemented in the VASP code[26] is used to obtain the electronic structure. The interaction between the valence electrons and the core electrons (and the atomic nuclei) is described with the projector augmented-wave (PAW) method.[27] The electronic and magnetic properties of LCMO depend strongly on the doping $x$. Theoretical EELS spectra for four values of $x$ have been calculated: the end-point compounds $CaMnO_3$ (CMO) ($x=0$) and $LaMnO_3$ (LMO) ($x=1$), and intermediate values $x=0.33$ and 0.50. The crystal structures of both CMO and LMO have *Pnma* symmetry, while their spin configurations are different: CMO is *G*-type antiferromagnetic (AFM); LMO is *A*-type AFM. For the two intermediate doping levels, the unit cells can be viewed as multiple *Pnma* cells. They are AFM with complex spin configurations.[28,29]

To obtain O-K-edge spectra, the O 1*s* electron is excited to the unoccupied states above the Fermi level, leaving behind a core hole. A proper treatment of the interaction between the valence electrons and the core hole is required for accurate EELS spectra. In semiconductors and insulators, such as Si and $SiO_2$, the electron core-hole interaction has been shown to strongly modify the theoretical EELS spectra.[30,31] The $Z+1$ approximation, where the localized core hole is approximated as an extra proton in the nucleus, is often used to describe the effects of a core hole.[30,32,33] The simple method of approximating O-K-edge spectra as projected density of states (PDOS) of $p$ symmetry on an oxygen site in a perfect crystal can be called the $Z$ approximation.[19,20] The $Z+1$ approximation is employed to obtain the O-K-edge spectra in LCMO. Compared to results from the $Z$ approximation, the inclusion of core-hole potential pulls the near-edge spectral features downward in energy and increases their intensity. In contrast to the cases of Si and $SiO_2$, the overall O-K spectra of LCMO from $Z$ and $Z+1$ approximations are quite similar, indicating weak electron-hole ($e$-$h$) interaction. The weak $e$-$h$ interaction can be understood from the electronic structure of LCMO: the empty states near the Fermi energy, where the excited electron from the near-edge spectra resides, are mostly Mn 3*d* states, which are separated spatially from the oxygen core hole. In addition, the screening effect from the filled O 2*s* and 2*p* orbitals also reduces the strength of O core hole. Thus, the O-K-edge spectra in LCMO are less affected by electron-hole interaction and they more directly probe the unoccupied electronic states of the crystal.

The calculated O-K-edge spectra of LCMO as a function of doping are shown in Fig. 1. The threshold energies are set to zero because the absolute excitation energy is not calculated in the $Z+1$ approximation. Gaussian broadening has been used with full width at half maximum (FWHM) of 1 eV in panel (a) and 2 eV in panel (b). For $x=0.33$ and 0.50, we used supercells with the appropriate number of La and Ca atoms and the O-K spectra were calculated for nonequivalent O sites. The final theoretical spectrum was a weighted average of the individual spectra. These spectra are shown in panels (a) and (b). In addition, we computed O-K spectra by

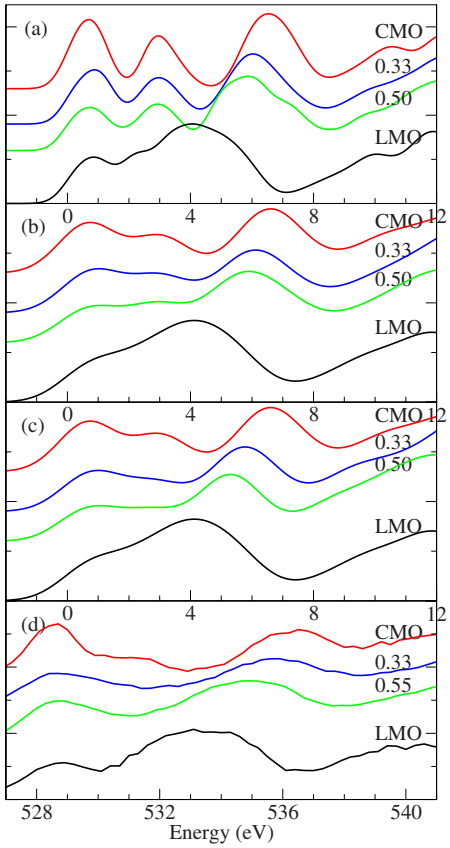


FIG. 1. (Color online) Theoretical and experimental O-K-edge EELS spectra of doped manganites LCMO. Calculated O-K-edge spectra broadened with a Gaussian function of (a) 1 and (b) 2 eV FWHM. (c) Calculated O-K-edge spectra broadened with a Gaussian function of 2 eV FWHM. Here "generic doping" is used for $x=0.33$ and 0.50. (d) Measured O-K-edge EELS spectra, adapted from Ref. 14. For the calculated spectra, the zero energy is set to the Fermi energy.

starting with CMO and introducing "generic doping;"[21] i.e., we introduce an appropriate number of extra electrons and compensate them with a uniform positive background. These spectra are broadened by 2 eV and are shown in panel (c). The experimental spectra are shown in panel (d). The most notable difference between the theoretical and experimental spectra is the resolution of the prepeak into two distinct peaks, which merge if sufficient broadening is included.

The calculated spectra exhibit two clear trends: (1) the energy width of the prepeaks decreases as the electron doping increases, from 4 eV in CMO to 2 eV in LMO; in addition, the intensity of the prepeak (area under the peak) relative to the main peak decreases as electron doping increases; (2) the energy separation between the prepeak and main peak also decreases as electron doping increases. Both the theoretical and experimental spectra show exactly the same trends as a function of doping.

It is common practice to extract quantitative measures of the prepeak intensities and the two-peak energy separation from experimental data and plot them against the nominal oxidation state of the cation. We used the same procedure, described in Ref. 14, to extract such quantitative measures

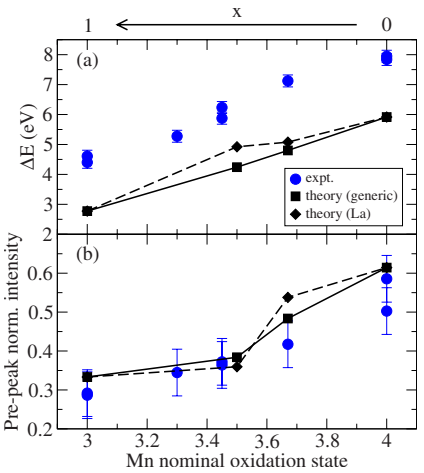


FIG. 2. (Color online) Comparison of the calculated and experimental EELS spectra features as a function of Mn nominal oxidation state in LCMO: (a) two-peak separation ($\Delta E$) and (b) normalized prepeak intensity (experimental data adapted from Ref. 14).

from both the experimental spectra and the 2-eV-broadened theoretical spectra of Fig. 1. The results are plotted in Fig. 2 against the Mn nominal oxidation state. The trends are in good agreement, with the only exception being the fact that theoretical peak separations are smaller than the experimental values. The effect is caused by the well-known feature of local-density approximations for exchange correlation to underestimate energy gaps and slightly compress the empty-state continuum.

The good agreement between the calculations and measured spectra provides a solid foundation for understanding the relationship between the O-K prepeak and oxidation state of TM ions. The PDOSs of the La/Ca and Mn atoms which are closest to the excited O site are analyzed. For CMO, the calculated prepeak has the same energy as the neighboring Mn 3*d* states, while the main peak coincides in energy with Ca 3*d* states, as shown in Fig. 3(a). With increasing doping of La, the calculated prepeak and main peak track the PDOS of neighboring atoms: the prepeak corresponds to Mn 3*d* states, and the main peak to La 5*d* and/or Ca 3*d* states, as shown in Figs. 3(b) and 3(c). This picture implies hybridization of O 2*p* states with Mn 3*d* and La 5*d* and/or Ca 3*d* states, which is consistent with previous studies of TMOs.[6,11]

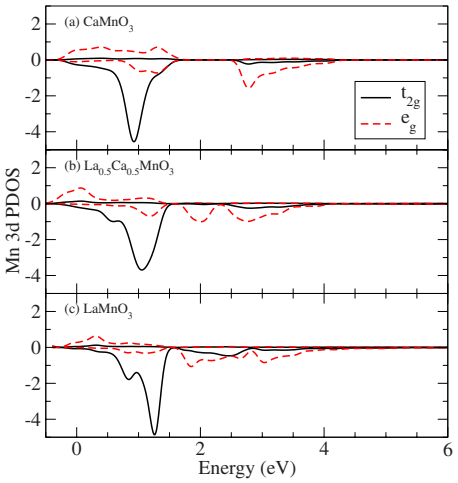


FIG. 4. (Color online) PDOS (unit: states/eV) of Mn 3*d* majority-spin and minority-spin $t_{2g}$ and $e_g$ orbitals in CMO, 50%-doped LCMO and LMO, showing the evolution of Mn 3*d* orbital occupancy and crystal-field splitting as a function of doping. Positive values correspond to majority-spin states, and negative values correspond to minority-spin states.

We further probe the effects of electronic and lattice properties on the evolution of the prepeak as a function of doping. In the simple picture of electron counting, which defines the nominal oxidation state, the $Mn^{4+}$ ion in CMO has $t_{2g}^3$ configuration in the majority spin, while the $Mn^{3+}$ ion in LMO has $t_{2g}^3 e_g^1$ configuration in the majority spin. For the Mn atom closest to the excited O site, the symmetry-decomposed unoccupied Mn 3*d* states ($t_{2g}$ and $e_g$) of both majority and minority spins are plotted in Fig. 4, for CMO, 50% doped LCMO and LMO. In the majority-spin channel, the intensity of the unoccupied $t_{2g}$ states is very small, while the intensity of the unoccupied $e_g$ states decreases as the electron doping increases, in agreement with the simple picture. The minority-spin states remain almost unchanged. The intensities of the unoccupied majority-spin $e_g$ states (PDOS integrated from 0 to 5 eV) are 0.98, 0.70, 0.53, and 0.44 for CMO, 33% doped, 50% doped, and LMO, respectively. These numbers show a clear trend of the prepeak intensity with doping that parallels the trend in Fig. 2 where the prepeak intensity is plotted against the Mn nominal oxidation

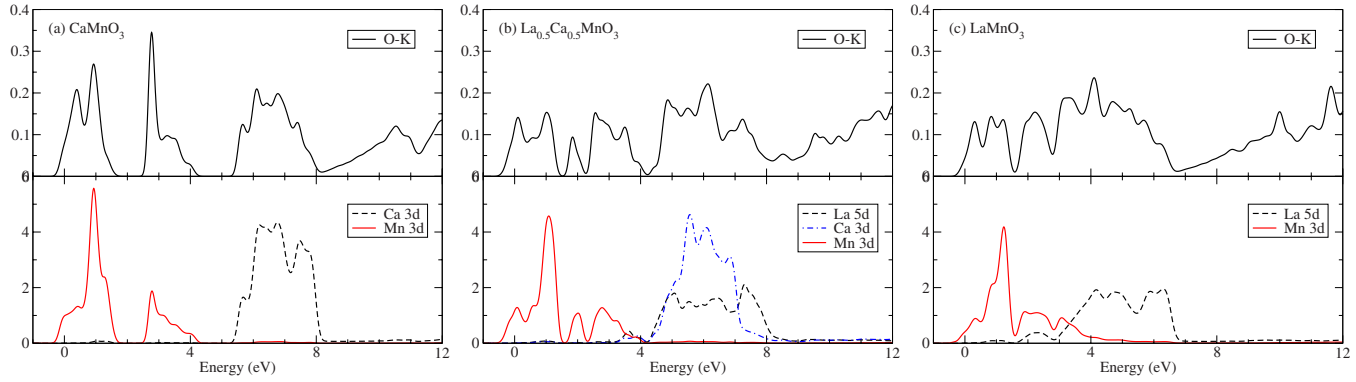


FIG. 3. (Color online) Theoretical O-K-edge EELS spectra from the $Z+1$ approximation (top panels) and PDOS (unit: states/eV) of Mn and Ca/La atoms that are the nearest neighbors of the excited O (bottom panels) in (a) $CaMnO_3$, (b) $La_{0.5}Ca_{0.5}MnO_3$, and (c) $LaMnO_3$.

state. Thus, the well-known correlation of the prepeak intensity with nominal oxidation state is explained by the results on orbital occupancies, confirming a conclusion reached in Ref. 21. We wish to emphasize that, despite the orbital-occupancy changes, the actual physical charge on Mn atoms remains unchanged with doping. In fact, as we showed quantitatively in Ref. 21, Mn atoms are effectively neutral in all cases.

In addition to the overall prepeak intensity variation with doping, the prepeak width decreases with increasing doping (Fig. 1). We found that the cause of this effect is the fact that the energy gap between the minority-spin $t_{2g}$ and $e_g$ states decreases when going from CMO to LMO. The cause of the decrease is the crystal-field splitting: LMO has larger Mn-O bond length, thus weaker crystal field, than CMO. Both the electronic and lattice effects control the O-K prepeak.

The dependence of the peak separation $\Delta E$ on the Mn nominal oxidation state (Fig. 2) can be understood as follows. Figure 3 show that the main peak tracks the position of the Ca $3d$ and La $5d$ states. The calculated energy ranges of the La $5d$ states indeed lie lower than those of the Ca $3d$ states, in accord with the data. Thus the true physical correlation of $\Delta E$ is with the doping variable $x$, shown on the top abscissa labeling of Fig. 2. The correlation of $\Delta E$ with nominal oxidation state, shown in the bottom abscissa labeling, arises simply because the nominal oxidation state is defined by $n=4-x$.

In conclusion, the theoretical results reported in this Brief Report confirm that the prepeak in O-K EELS spectra of manganites measures the electronic occupancy of the hybridized O $2p$ and Mn $3d$ states. Thus the prepeak intensity is related to the *nominal* oxidation state of the Mn, not the real charge on Mn or O sites. Lattice effects also play a role in the structure of the O-K EELS through crystal-field splitting: higher electron doping means longer Mn-O bonds and weaker crystal-field splitting, resulting in smaller width for the O-K prepeak. The empirical method of using O-K prepeak to probe TM oxidation states is now on firmer ground. The energy separation between the prepeak and the main peak has a correlation with the doping parameter $x$, which translates into a correlation with the nominal oxidation because the latter is defined by $n=4-x$.

Research was sponsored by the DOE Office of Basic Energy Sciences, Division of Materials Sciences and Engineering, and by the McMinn Endowment at Vanderbilt University. Computations were performed at the National Energy Research Scientific Computing Center.

[1] S. Jin, T. H. Tiefel, M. Mccormack, R. A. Fastnacht, R. Ramesh, and L. H. Chen, Science **264**, 413 (1994).
[2] P. Schiffer, A. P. Ramirez, W. Bao, and S. W. Cheong, Phys. Rev. Lett. **75**, 3336 (1995).
[3] M. Imada, A. Fujimori, and Y. Tokura, Rev. Mod. Phys. **70**, 1039 (1998).
[4] E. Dagotto, T. Hotta, and A. Moreo, Phys. Rep. **344**, 1 (2001).
[5] E. Dagotto, Science **309**, 257 (2005).
[6] M. Abbate, F. M. F. de Groot, J. C. Fuggle, A. Fujimori, O. Strebel, F. Lopez, M. Domke, G. Kaindl, G. A. Sawatzky, M. Takano, Y. Takeda, H. Eisaki, and S. Uchida, Phys. Rev. B **46**, 4511 (1992).
[7] H. Kurata, E. Lefevre, C. Colliex, and R. Brydson, Phys. Rev. B **47**, 13763 (1993).
[8] H. L. Ju, H. C. Sohn, and K. M. Krishnan, Phys. Rev. Lett. **79**, 3230 (1997).
[9] F. M. F. de Groot, M. Grioni, J. C. Fuggle, J. Ghijsen, G. A. Sawatzky, and H. Petersen, Phys. Rev. B **40**, 5715 (1989).
[10] M. Abbate, J. C. Fuggle, A. Fujimori, L. H. Tjeng, C. T. Chen, R. Potze, G. A. Sawatzky, H. Eisaki, and S. Uchida, Phys. Rev. B **47**, 16124 (1993).
[11] G. Zampieri, F. Prado, A. Caneiro, J. Briatico, M. T. Causa, M. Tovar, B. Alascio, M. Abbate, and E. Morikawa, Phys. Rev. B **58**, 3755 (1998).
[12] M. Varela, A. R. Lupini, V. Pena, Z. Sefrioui, I. Arslan, N. D. Browning, J. Santamaria, and S. J. Pennycook, arXiv:cond-mat/0508564 (unpublished).
[13] M. Varela, A. R. Lupini, K. van Benthem, A. Y. Borisevich, M. F. Chisholm, N. Shibata, E. Abe, and S. J. Pennycook, Annu. Rev. Mater. Res. **35**, 539 (2005).
[14] M. Varela, M. P. Oxley, W. Luo, J. Tao, M. Watanabe, A. R. Lupini, S. T. Pantelides, and S. J. Pennycook, Phys. Rev. B **79**, 085117 (2009).
[15] J. Graetz, C. C. Ahn, R. Yazami, and B. Fultz, J. Phys. Chem. B **107**, 2887 (2003).
[16] F. M. F. de Groot, J. Faber, J. J. M. Michiels, M. T. Czyzyk, M. Abbate, and J. C. Fuggle, Phys. Rev. B **48**, 2074 (1993).
[17] L. A. Grunes, R. D. Leapman, C. N. Wilker, R. Hoffmann, and A. B. Kunz, Phys. Rev. B **25**, 7157 (1982).
[18] J. van Elp and A. Tanaka, Phys. Rev. B **60**, 5331 (1999).
[19] S. Miao, M. Kocher, P. Rez, B. Fultz, Y. Ozawa, R. Yazami, and C. C. Ahn, J. Phys. Chem. B **109**, 23473 (2005).
[20] J. Graetz, A. Hightower, C. C. Ahn, R. Yazami, P. Rez, and B. Fultz, J. Phys. Chem. B **106**, 1286 (2002).
[21] W. Luo, A. Franceschetti, M. Varela, J. Tao, S. J. Pennycook, and S. T. Pantelides, Phys. Rev. Lett. **99**, 036402 (2007).
[22] H. Raebiger, S. Lany, and A. Zunger, Nature (London) **453**, 763 (2008).
[23] P. Hohenberg and W. Kohn, Phys. Rev. **136**, B864 (1964).
[24] W. Kohn and L. J. Sham, Phys. Rev. **140**, A1133 (1965).
[25] J. P. Perdew, K. Burke, and M. Ernzerhof, Phys. Rev. Lett. **77**, 3865 (1996).
[26] G. Kresse and J. Furthmüller, Phys. Rev. B **54**, 11169 (1996).
[27] P. E. Blöchl, Phys. Rev. B **50**, 17953 (1994).
[28] P. G. Radaelli, D. E. Cox, M. Marezio, and S. W. Cheong, Phys. Rev. B **55**, 3015 (1997).
[29] P. G. Radaelli, D. E. Cox, L. Capogna, S. W. Cheong, and M. Marezio, Phys. Rev. B **59**, 14440 (1999).
[30] R. Buczko, G. Duscher, S. J. Pennycook, and S. T. Pantelides, Phys. Rev. Lett. **85**, 2168 (2000).
[31] G. Duscher, R. Buczko, S. J. Pennycook, and S. T. Pantelides, Ultramicroscopy **86**, 355 (2001).
[32] T. Fujikawa, J. Phys. Soc. Jpn. **52**, 4001 (1983).
[33] C. Elsasser and S. Kostlmeier, Ultramicroscopy **86**, 325 (2001).